Nuclear structure with exotic beams

Lecture 2:

Nuclear reactions I

Elastic and Inelastic Scattering

A. Wuosmaa
University of Connecticut
Department of Physics

CNSSS19 Japan

Some types of collisions

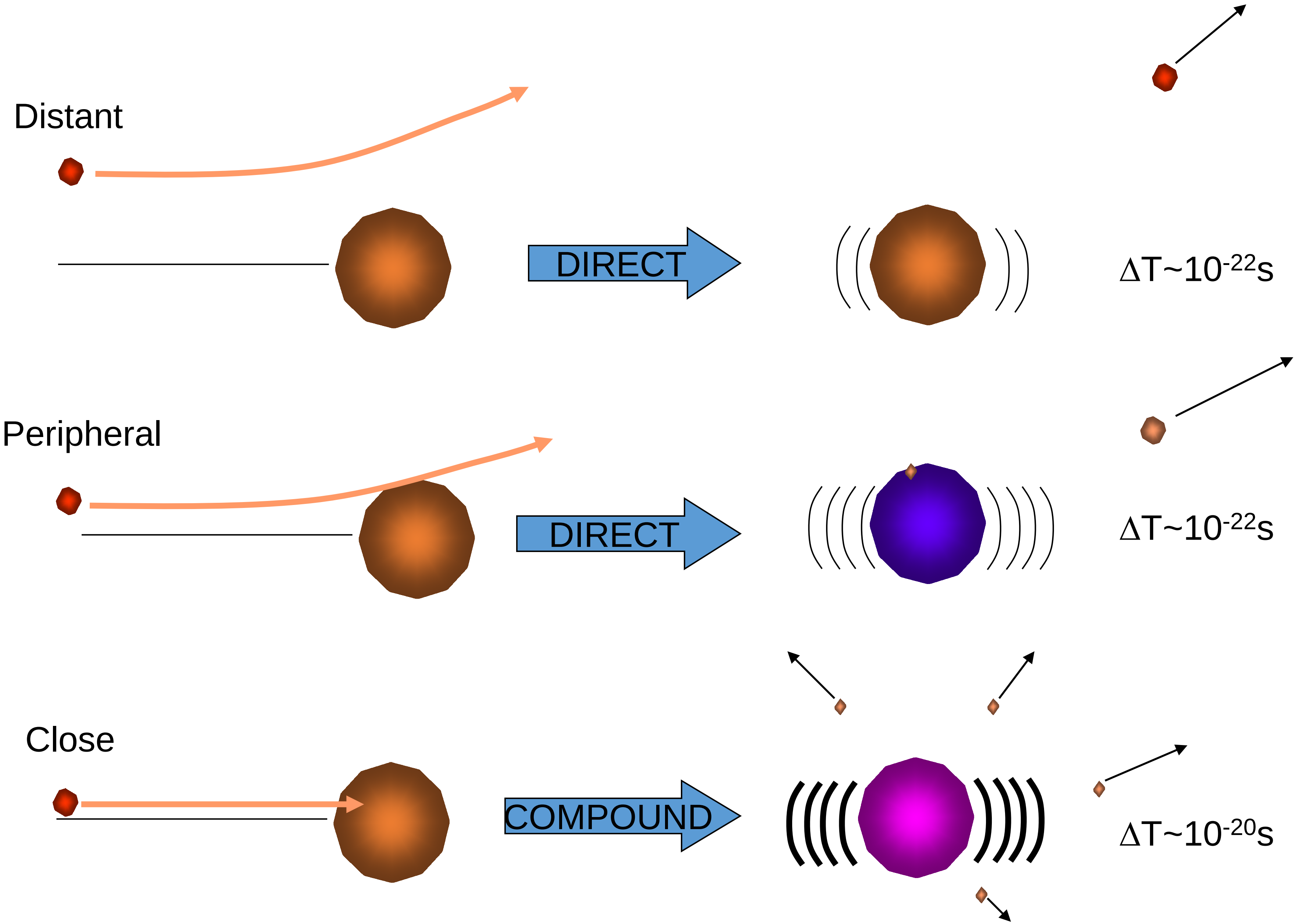

Very simple measurements can tell us important things

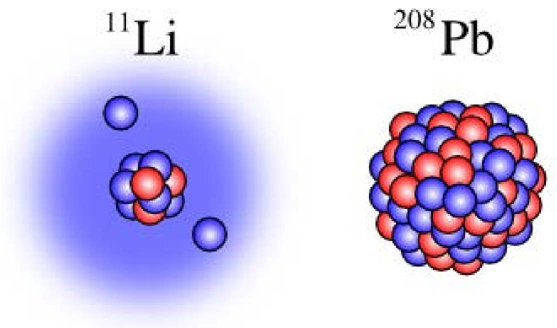

TABLE I. Interaction cross sections (σ_I) in millibarns.

Beam	Target Be	Target C	Target Al
^{6}Li	651 ± 6	688 ± 10	1010 ± 11
^{7}Li	686 ± 4	736 ± 6	1071 ± 7
^{8}Li	727 ± 6	768 ± 9	1147 ± 14
^{9}Li	739 ± 5	796 ± 6	1135 ± 7
^{11}Li		1040 ± 60	
^{7}Be	682 ± 6	738 ± 9	1050 ± 17
^{9}Be	755 ± 6	806 ± 9	1174 ± 11
^{10}Be	755 ± 7	813 ± 10	1153 ± 16

First experimental hint that ^{11}Li was special – simply a total interaction cross section

I. Tanihata et al, PRL **55**, 2676 (1985)

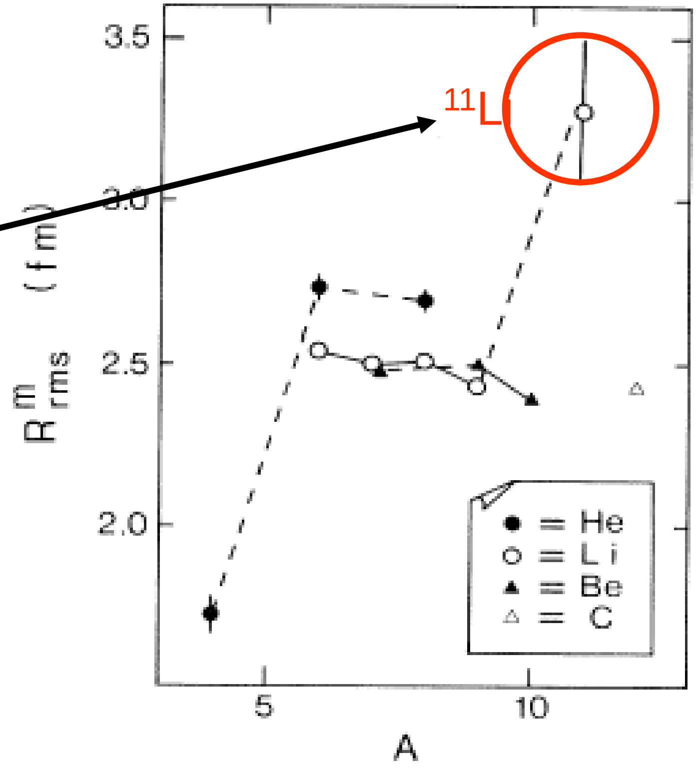

FIG. 3. Matter rms radius R^m_{rms}. Lines connecting isotopes are only guides for the eye. Differences in radii are seen for isobars with $A = 6$, 8, and 9. The ^{11}Li isotope has a much larger radius than other nuclei.

Coulomb trajectories

Lower energy –
does not penetrate nucleus

Distant trajectory
(Important for Coulomb Excitation later on)

Peripheral Trajectory
(Important for nucleon transfer later on)

Close collision

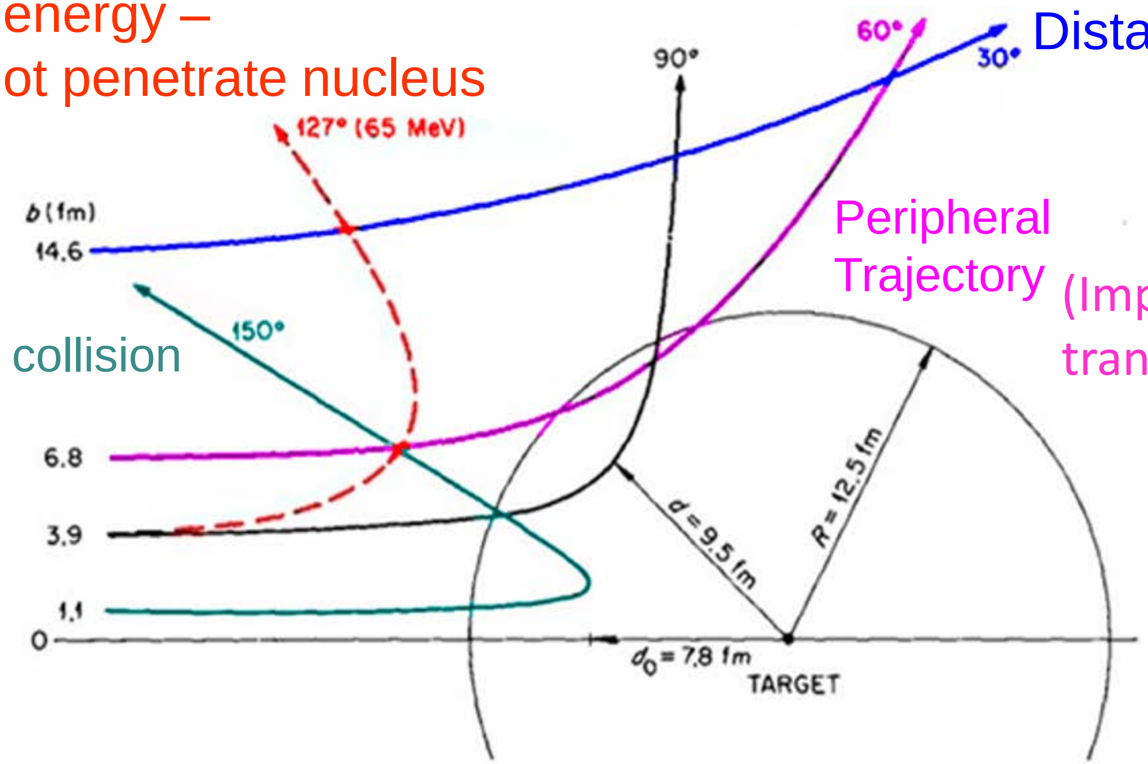

"Grazing angle":
angle corresponding to the trajectory for which the two nuclei just touch each other

$^{16}O + ^{208}Pb$ $E(^{16}O) = 130$ MeV, $V_C \sim 93$ MeV

(Satchler, *Direct Nuclear Reactions* 1980, pp 36)

Schematic evolution of elastic scattering with energy and angle

Low energy/large impact parameter -
1 dominant trajectory
$d\sigma/d\Omega \sim d\sigma_R/d\Omega$

$\theta<\theta_{GR}$
$b>R_{12}$

Grazing trajectories from either side interfere constructively – "Fresnel" or "Coulomb-nuclear" interference and $d\sigma/d\Omega > d\sigma_R/d\Omega$

$\theta\sim\theta_{GR}$
$b\sim R_{12}$

Higher energy/small impact parameter:
absorption, 2 interfering trajectories:
$d\sigma/d\Omega<<d\sigma_R/d\sigma$

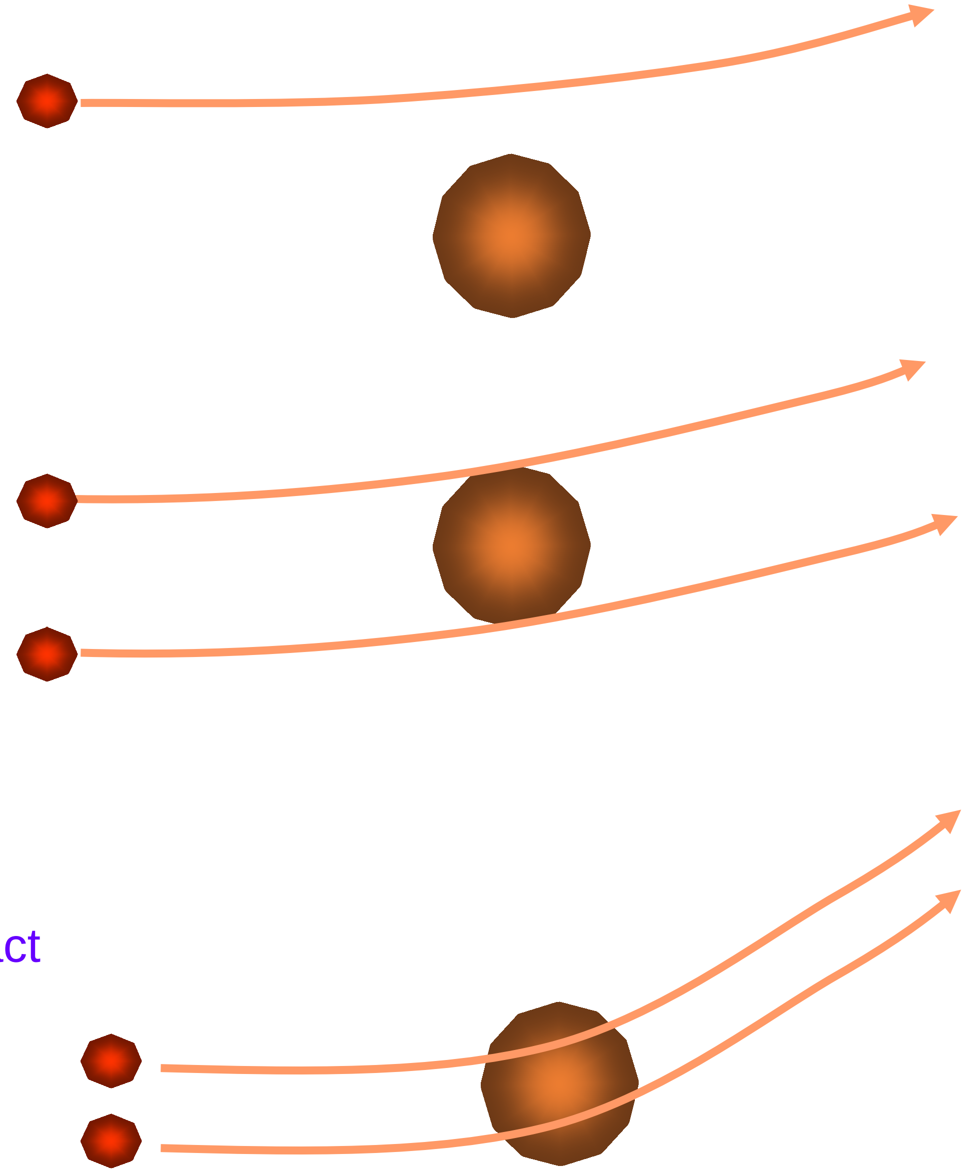

$\theta>\theta_{GR}$
$b<R_{12}$

Evolution of elastic-scattering angular distributions with energy

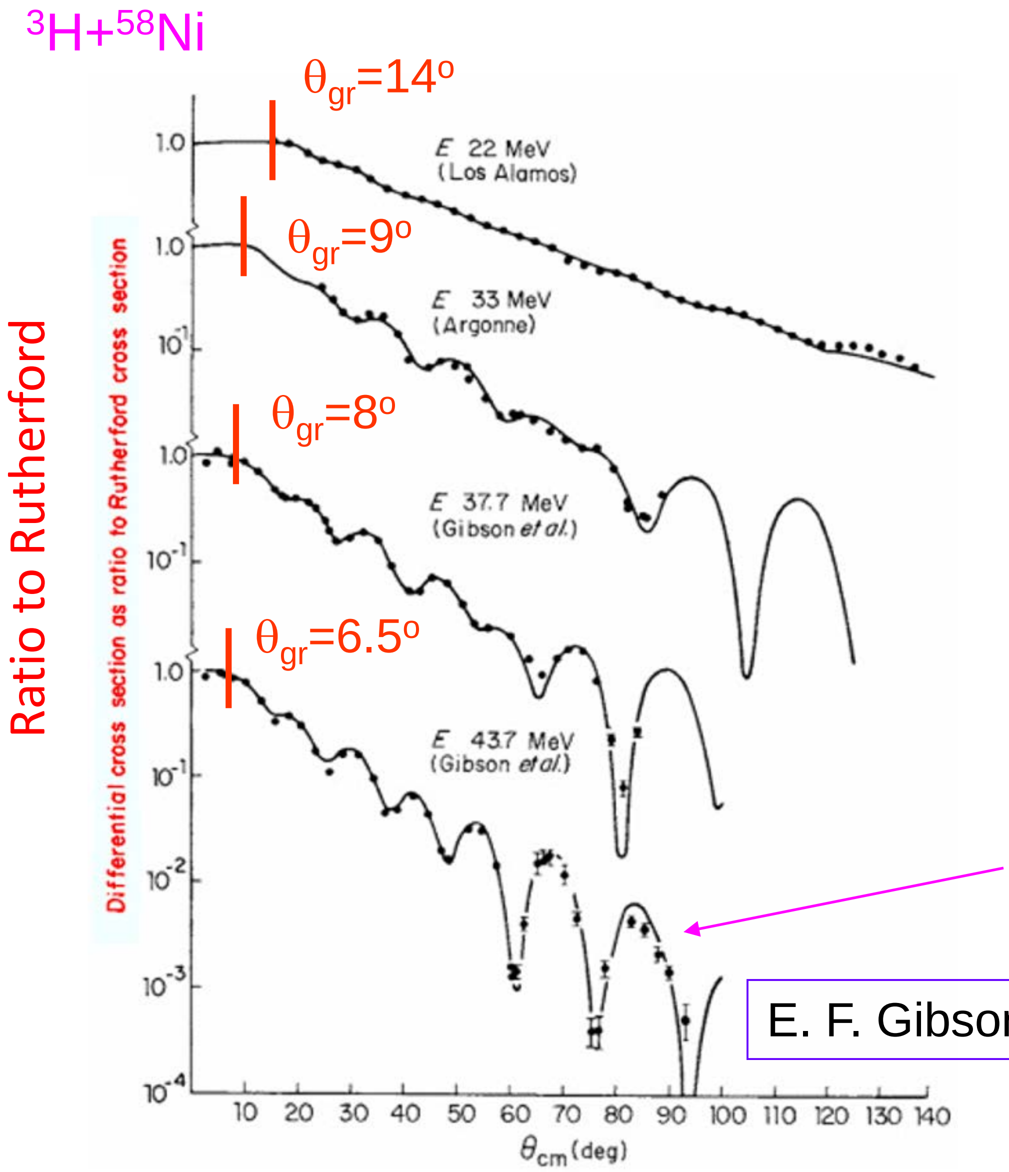

E. F. Gibson, PR **155**, 1208 (1967)

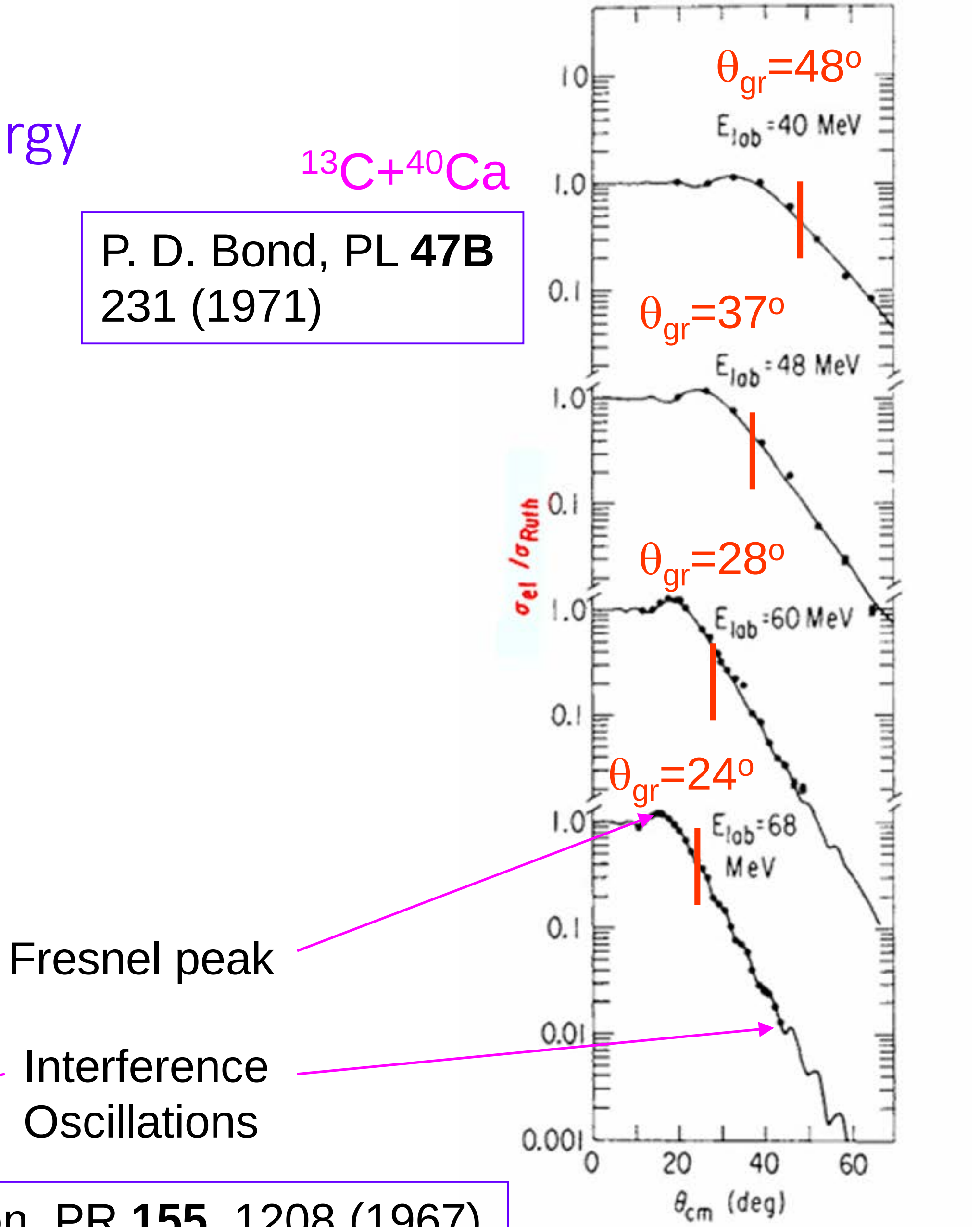

P. D. Bond, PL **47B** 231 (1971)

Figs. from Glendenning 2004, pp 38 and 39

The Optical Model

- The optical model is a schematic model of nuclear scattering that sweeps all of the microscopic nuclear structure under the rug.

- It is called “optical” because it treats the incident and outgoing particles as waves scattered by some ~spherical region. Those waves can also be absorbed (“cloudy ball”) and we can lose flux (particles), thus reducing the elastic scattering cross section.

- The combined effects of many complex states are averaged into a single nucleus-nucleus potential – called the Optical Potential

Formalism and Optical Model scattering

Need a solution to Schrödinger's equation

$$-\frac{\hbar^2}{2m}\frac{d^2u_l(r)}{dr^2}+\left[U(r)+\frac{\hbar^2}{2m}\frac{l(l+1)}{r^2}\right]u_l(r)=Eu_l(r)$$

The asymptotic solutions are waves and an approximate (Born) solution is:

$$\frac{d\sigma}{d\Omega}=\left|f(\theta,\phi)\right|^2;\quad f(\theta,\phi)=-\frac{1}{4\pi}\int\exp(-i\vec{k}'\cdot\vec{r}')U(r')\exp(i\vec{k}\cdot\vec{r}')dr'$$

A better treatment uses asymptotic solutions that are waves distorted by the Coulomb Potential:

"Distorted-Wave Born Approximation" or DWBA

U(r) is the Optical Potential, consisting of:

Volume, surface, and $\boldsymbol{l}\cdot\boldsymbol{S}$ (real and imaginary)

Contributions to $U(r)$

- Coulomb part: $V_C(r) = Z_1 Z_2 e^2/r$
- Real Nuclear part: $V(r)$
  - Comes from the nuclear attraction
- Imaginary Nuclear Part (!): $W(r)$
  - Why? Other things can happen so we can lose elastic flux! There must be "absorption" of waves.
- Spin-Orbit ($\boldsymbol{l} \cdot \boldsymbol{S}$) part: $V_{SO}(r)$
  - Why? There is a spin-orbit component to the nuclear force so it seems natural to have one between nuclei. Also, it seems to be needed to explain polarization data!

$$U(r)=V_C(r) + V(r) + iW(r) + V_{SO}(r)$$

Only the real parts contribute to elastic scattering

Volume and surface potentials

$R=r_0(A_1^{1/3}+A_2^{1/3})$ is the radius where the potential is ½ its maximum.

"a" is the "diffuseness" parameter. It describes the "spread" of the potential about R.

Typically, the spin-orbit potential is described as

$$V_{SO} = \frac{C}{r}\frac{dg(r)}{dr}\vec{l}\cdot\vec{s}$$

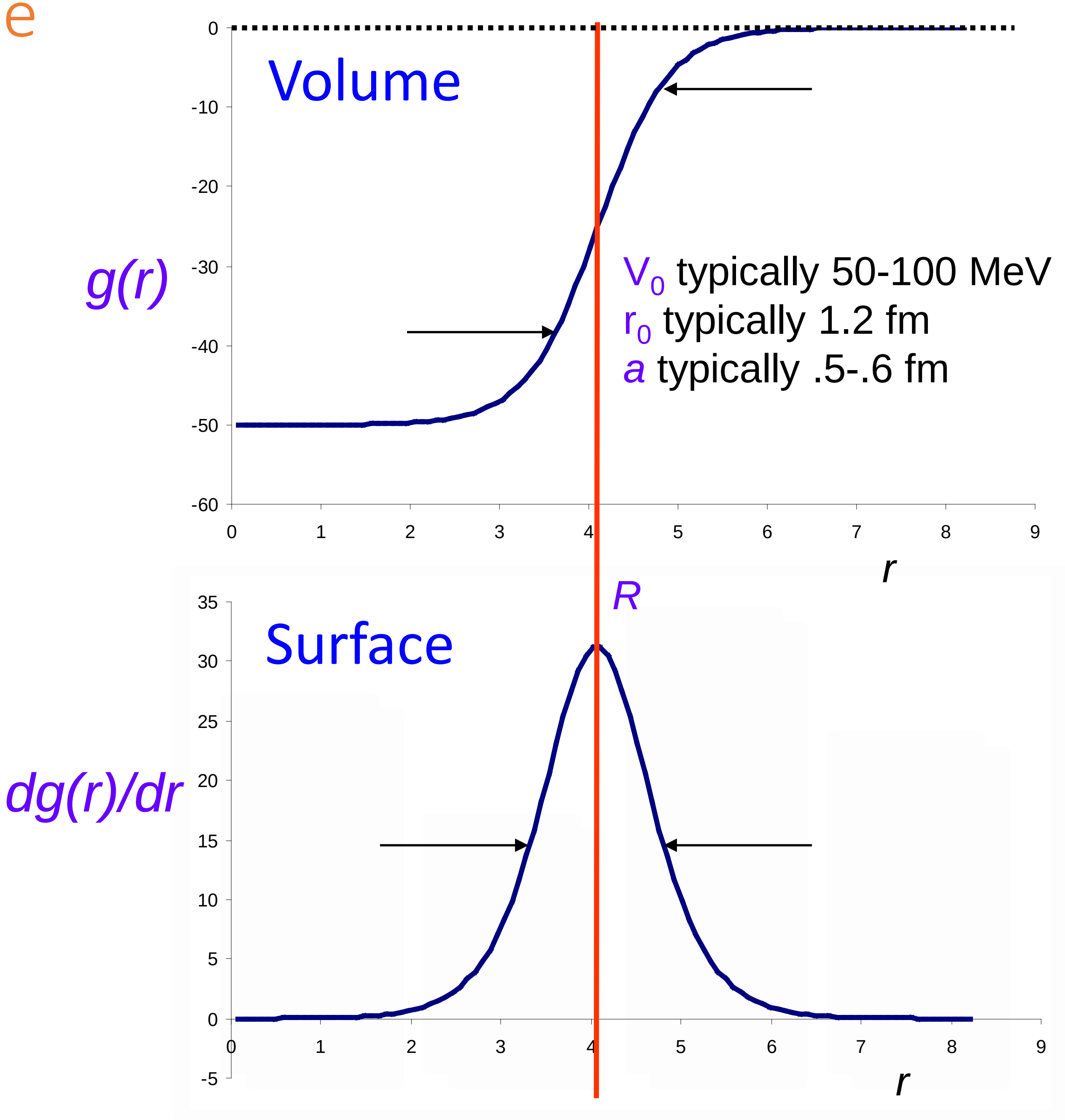

Inelastic scattering and channel coupling

Optical potential

Coupled differential equations

Coupling potential

$$(E_\alpha - T_{\alpha l} - U_\alpha)u_\alpha^0 = 0$$
$$(E_{\alpha'} - T_{\alpha l} - U_\alpha)u_{\alpha'}^0 = V_{\alpha\alpha'}u_\alpha^0$$

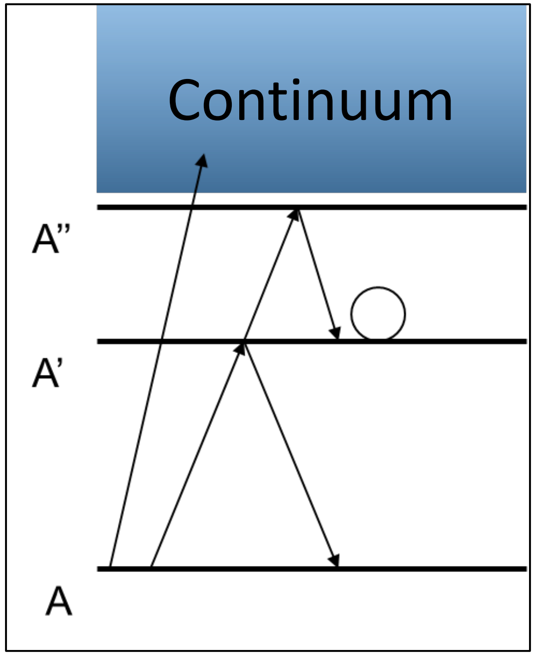

$$V_{\alpha\alpha'} \sim \langle \phi_{\alpha'} | V_{INEL}(r) | \phi_\alpha \rangle$$

ϕ_α are the intrinsic states in a collective model, and V_{INEL} is a coupling potential

$$V_{VIB}(r) \sim R_0 \frac{dU}{dr} \alpha_{\lambda\mu} Y_{\lambda\mu}^* (\vec{r})$$ Vibrational model

$$V_{ROT}(r) \sim R_0 \frac{dU}{dr} \beta_L Y_{LM} (\vec{r})$$ Rotational model

These correspond to distortions of the nuclear surface.

The α's and β's tell us about the collectivity of the nuclei

The β_L in particular give the magnitude of different multipole deformations

Coupling to rotational states

$\alpha + ^{154}Sm$

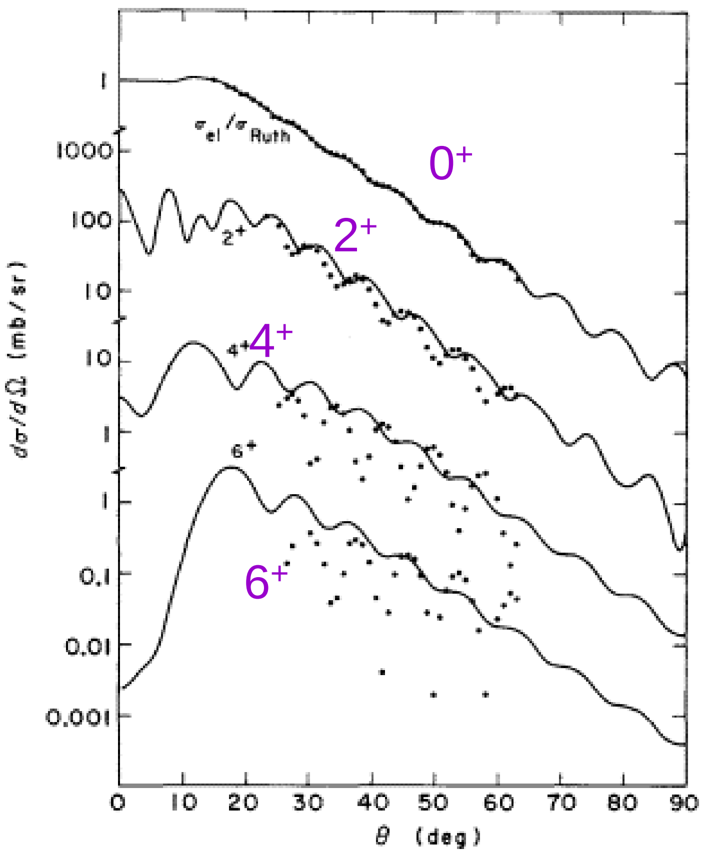

Fig. 13.3. Distorted-wave calculation with optical parameters that fit the elastic section as shown (listed in Chapter 4). $\beta_2 = 0.3$, $\beta_4 = 0.15$, $\beta_6 = 0.075$. DWBA, ^{154}Sm (Glendenning, 1969a).

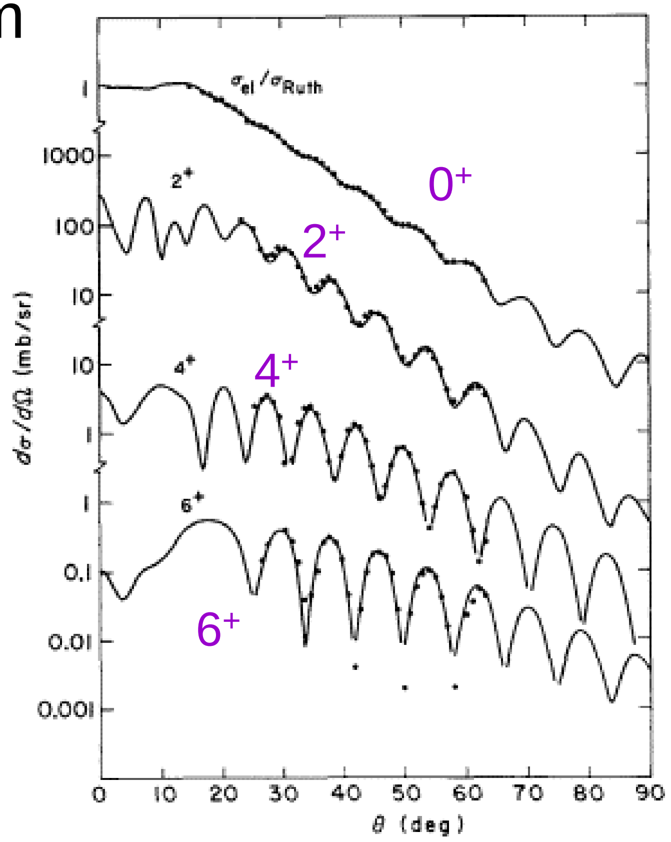

Fig. 13.4. Cross sections for 50-MeV alpha-excitation ground-state rotational band ^{154}Sm. Curves are coupled-channel calculation as described in text. The data were taken at tl Berkeley 88-in. Cyclotron. $\beta_2 = 0.225$, $\beta_4 = 0.05$, $\beta_6 = -0.015$ (from Harvey *et al.*, 196 Hendrie *et al.* 1968; calculation by Glendenning 1969a).

Elastic scattering alone can be fit with an optical model...

Channel-coupling is needed to fit the inelastic channels. Everything is treated simultaneously.

Continuum coupling: $^{11}Be+^{64}Zn$

Elastic scattering and Coupled Channels

DiPietro et al., PRC **85** 054607 (2012).

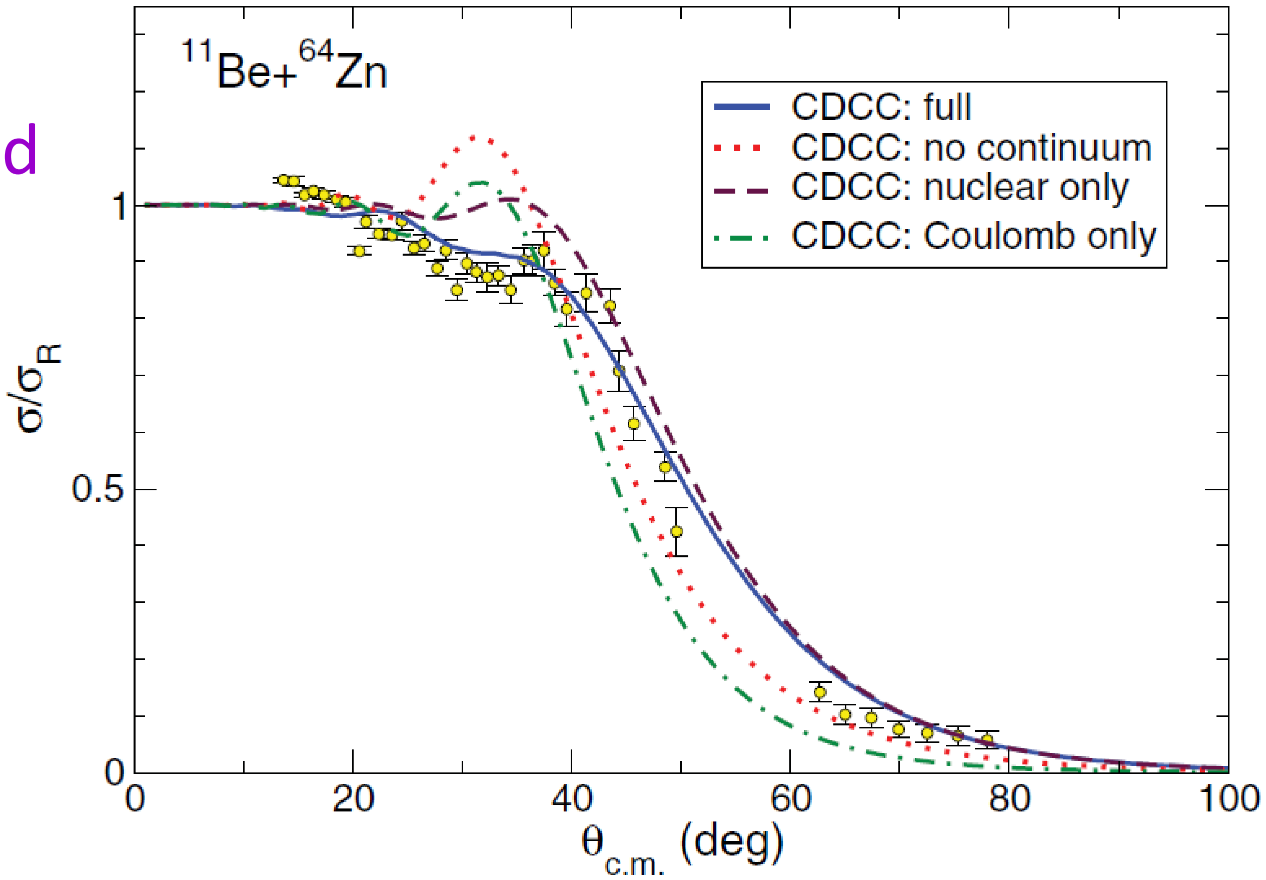

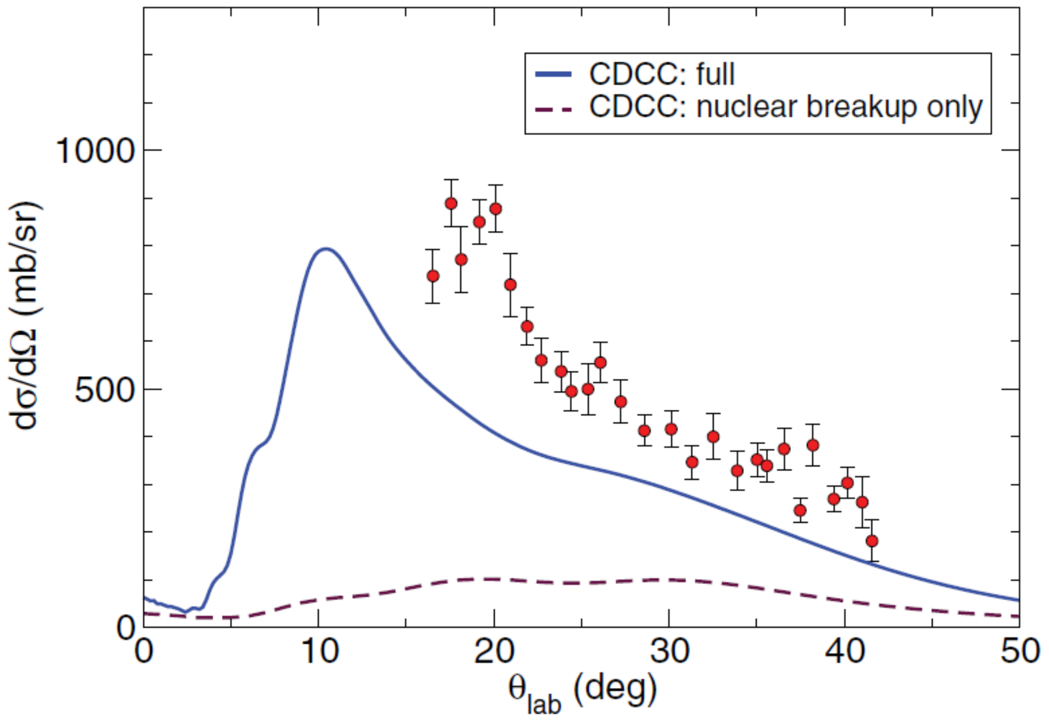

Breakup events and Coupled Channels

Continuum Discretized Coupled Channels

^{16}C+proton scattering

PHYSICAL REVIEW C **73**, 024610 (2006)

Neutron-dominant quadrupole collective motion in ^{16}C

H. J. Ong,[1,*] N. Imai,[2] N. Aoi,[2] H. Sakurai,[1] Zs. Dombrádi,[3] A. Saito,[4] Z. Elekes,[2,3] H. Baba,[4] K. Demichi,[5] Z. S. Fülöp,[3] J. Gibelin,[5,6] T. Gomi,[2] H. Hasegawa,[5] M. Ishihara,[2] H. Iwasaki,[1] S. Kanno,[5] S. Kawai,[5] T. Kubo,[2] K. Kurita,[5] Y. U. Matsuyama,[5] S. Michimasa,[2] T. Minemura,[2] T. Motobayashi,[2] M. Notani,[4,†] S. Ota,[7] H. K. Sakai,[5] S. Shimoura,[4] E. Takeshita,[5] S. Takeuchi,[2] M. Tamaki,[4] Y. Togano,[5] K. Yamada,[2] Y. Yanagisawa,[2] and K. Yoneda[2]

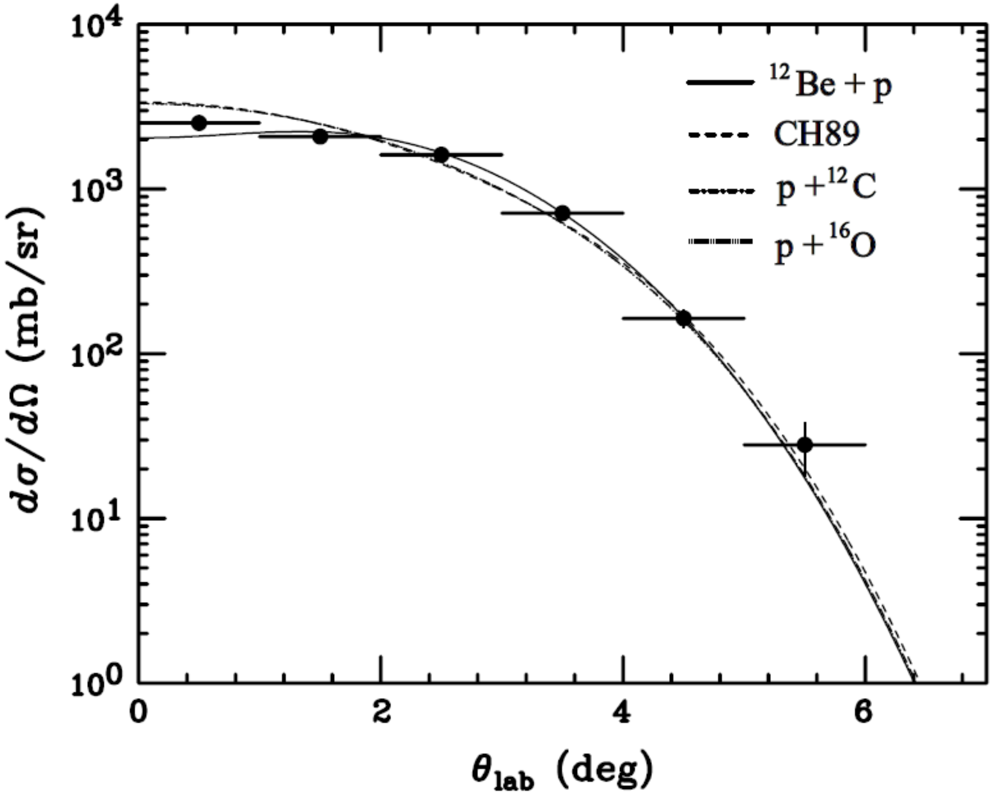

TABLE I. Nuclear deformation parameter $\beta_{pp'}$ and deformation length $\delta_{pp'}$ deduced from DWBA calculations.

Optical potential	$\beta_{pp'}$	r_0 (fm)	$\delta_{pp'}$ (fm)
CH89 [14]	0.476(37)	1.16	1.39(11)
p+^{16}O [15]	0.440(33)	1.14	1.26(9)
p+^{12}C [15]	0.531(42)	1.10	1.47(12)
^{12}Be+p [16]	0.435(32)	1.48	1.62(12)

$$\frac{M_n}{M_p} = \frac{b_p}{b_n}\left[\frac{\delta_{pp'}}{\delta_{em}}\left(1+\frac{b_n}{b_p}\frac{N}{Z}\right)-1\right]$$

Large ratio of M_n/M_p indicates particular sensitivity to neutron motion

M_p, M_n: proton and neutron matrix elements

b_p,b_n: proton and neutron interaction strengths

^{22}O-proton scattering

PRL 96, 012501 (2006) PHYSICAL REVIEW LETTERS week ending 13 JANUARY 2006

$N = 14$ Shell Closure in ^{22}O Viewed through a Neutron Sensitive Probe

E. Becheva,[1] Y. Blumenfeld,[1] E. Khan,[1] D. Beaumel,[1] J. M. Daugas,[2] F. Delaunay,[1] Ch-E. Demonchy,[3] A. Drouart,[4] M. Fallot,[1] A. Gillibert,[4] L. Giot,[3] M. Grasso,[1,5] N. Keeley,[4] K. W. Kemper,[6] D. T. Khoa,[7] V. Lapoux,[4] V. Lima,[1] A. Musumarra,[5] L. Nalpas,[4] E. C. Pollacco,[4] O. Roig,[2] P. Roussel-Chomaz,[3] J. E. Sauvestre,[2] J. A. Scarpaci,[1] F. Skaza,[4] and H. S. Than[7]

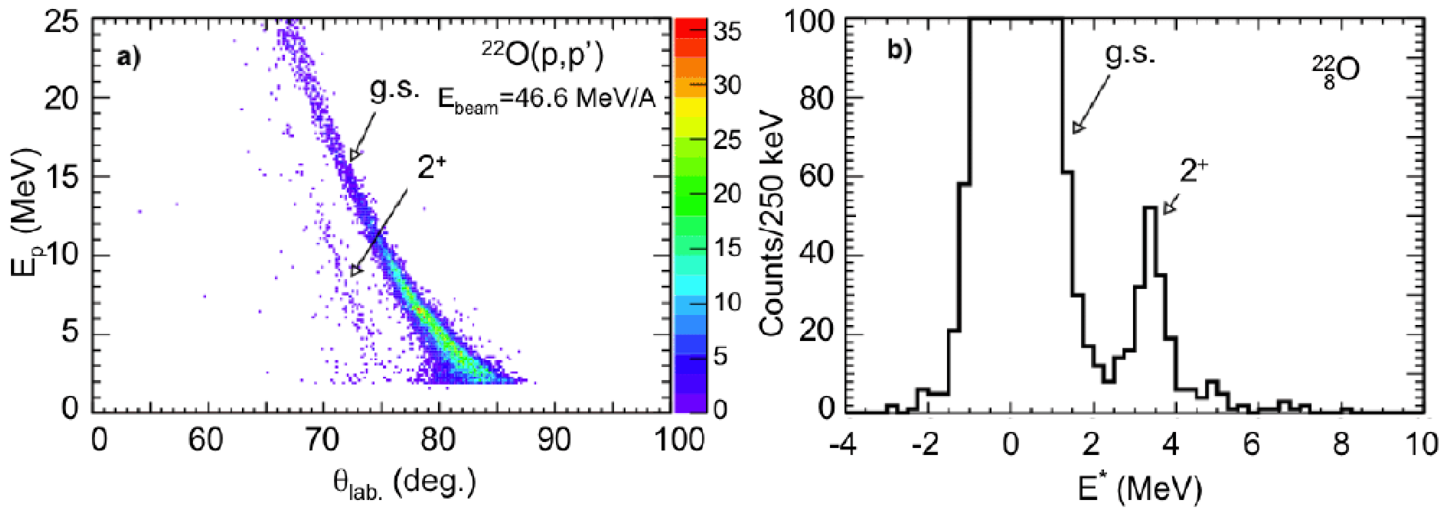

FIG. 1 (color online). (a) Scatter plot of recoiling proton energy versus scattering angle in the laboratory frame for the ^{22}O beam. (b) ^{22}O excitation energy spectrum deduced from the proton kinematics.

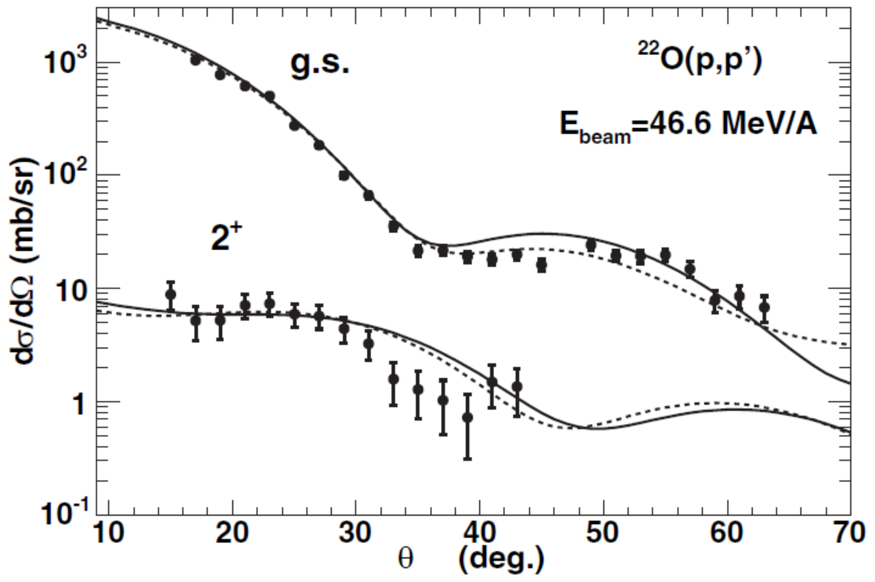

FIG. 2. Elastic and 2_1^+ inelastic angular distributions of ^{22}O at 46.6 A MeV (dots). DWBA using the phenomenological KD global optical potential (solid lines) and folding model (dashed lines) calculations are shown (see text).

Coulomb Excitation as a spectroscopic tool

	^{58}Ni^{a}	^{56}Ni	^{54}Ni
	Experimental results		
E_γ (keV)	1453(8)	2695(15)	1396(9)
σ (mb)	175(36)	107(26)	134(36)
v/c (midtarget)	0.373	0.391	0.346
θ_{lab}^{max} (degrees)	3.2	2.9	3.5
b_{min} (fm)	13.9	14.3	16.2
$B(E2\uparrow)$ (e^2 fm^4)	707(145)	494(119)	626(169)
	Adopted values		
E_γ (keV)	1454.28(10)	2700.6(7)	
$B(E2\uparrow)$ (e^2 fm^4)	695(20)	600(120)	

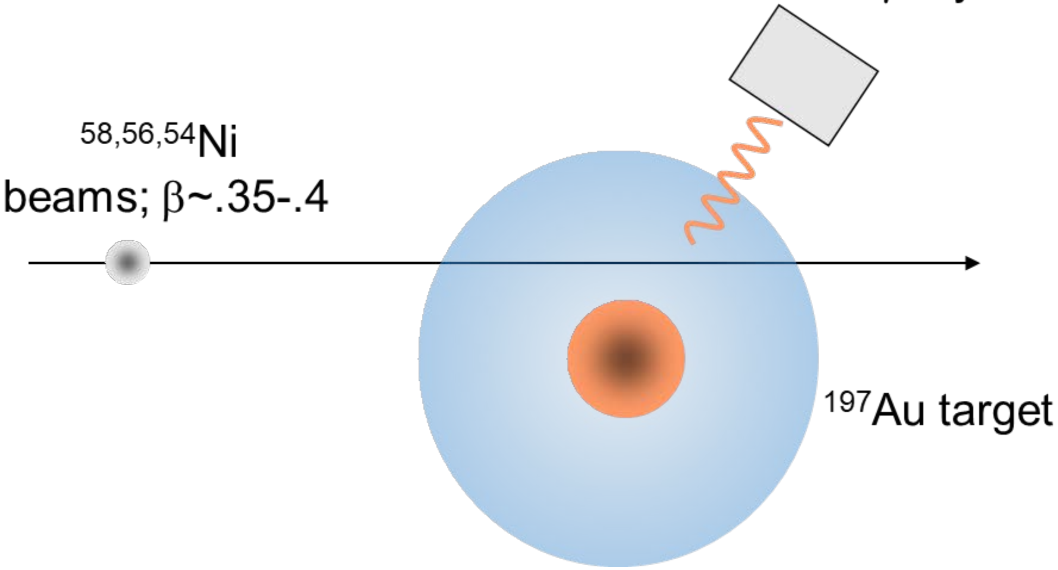

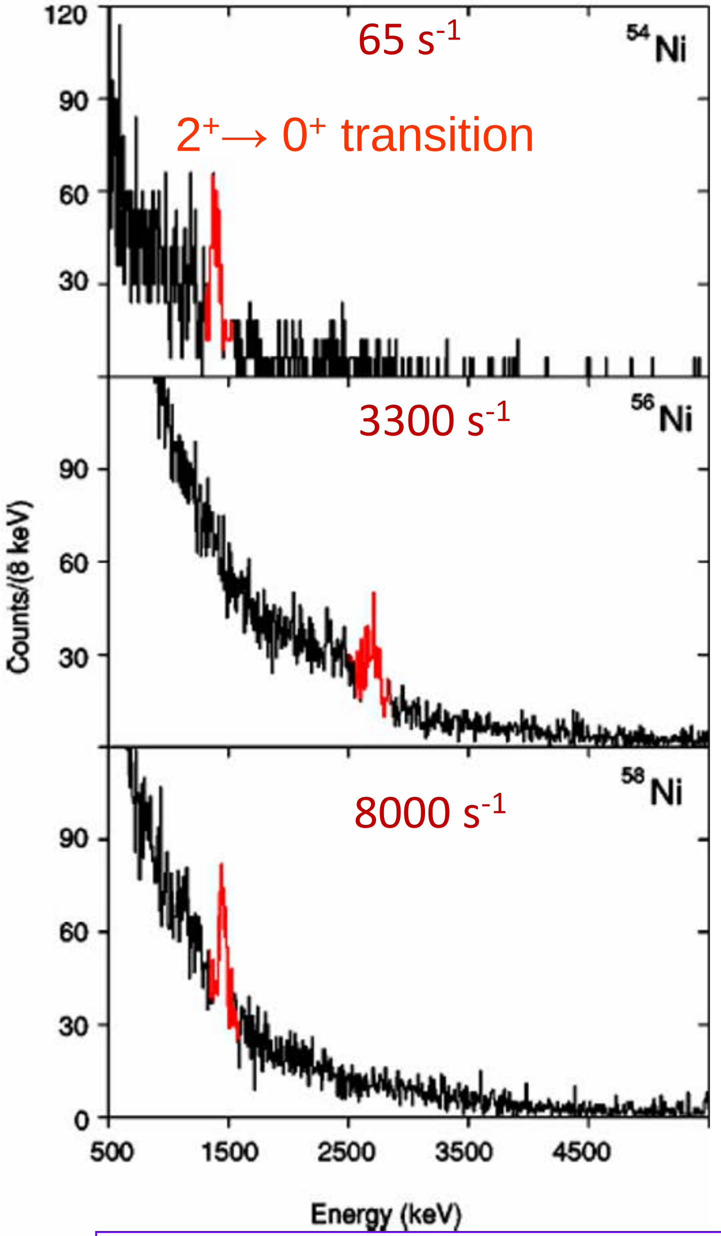

K. L Yurkewicz et al, PRC **70**, 054319 (2004)

SEGA(MSU, 2004) and GRETINA (Now)

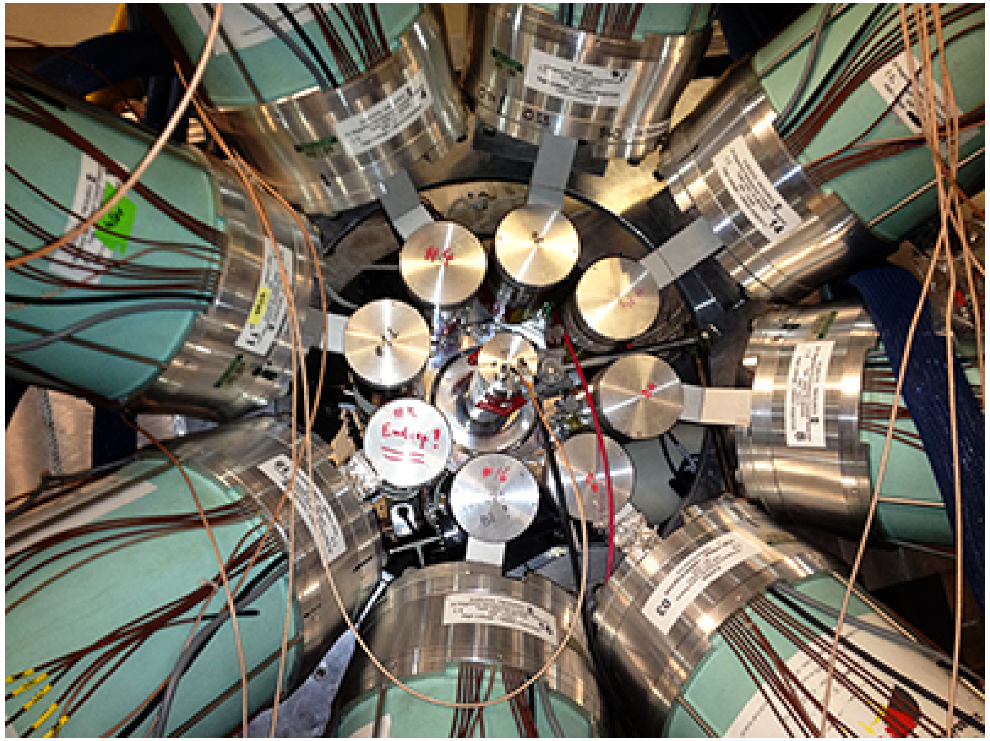

SEGA MSU Circa 2004

GRETINA circa 2017

Coulomb excitation and octupole deformation

PRL 118, 152504 (2017) PHYSICAL REVIEW LETTERS week ending 14 APRIL 2017

Direct Evidence for Octupole Deformation in ^{146}Ba and the Origin of Large $E1$ Moment Variations in Reflection-Asymmetric Nuclei

B. Bucher,[1,2,*] S. Zhu,[3,†] C. Y. Wu,[1] R. V. F. Janssens,[3] R. N. Bernard,[4] L. M. Robledo,[4] T. R. Rodríguez,[4] D. Cline,[5] A. B. Hayes,[5] A. D. Ayangeakaa,[3] M. Q. Buckner,[1] C. M. Campbell,[6] M. P. Carpenter,[3] J. A. Clark,[3] H. L. Crawford,[6] H. M. David,[3,‡] C. Dickerson,[3] J. Harker,[3,7] C. R. Hoffman,[3] B. P. Kay,[3] F. G. Kondev,[3] T. Lauritsen,[3] A. O. Macchiavelli,[6] R. C. Pardo,[3] G. Savard,[3] D. Seweryniak,[3] and R. Vondrasek[3]

~3000 ^{146}Ba s^{-1}

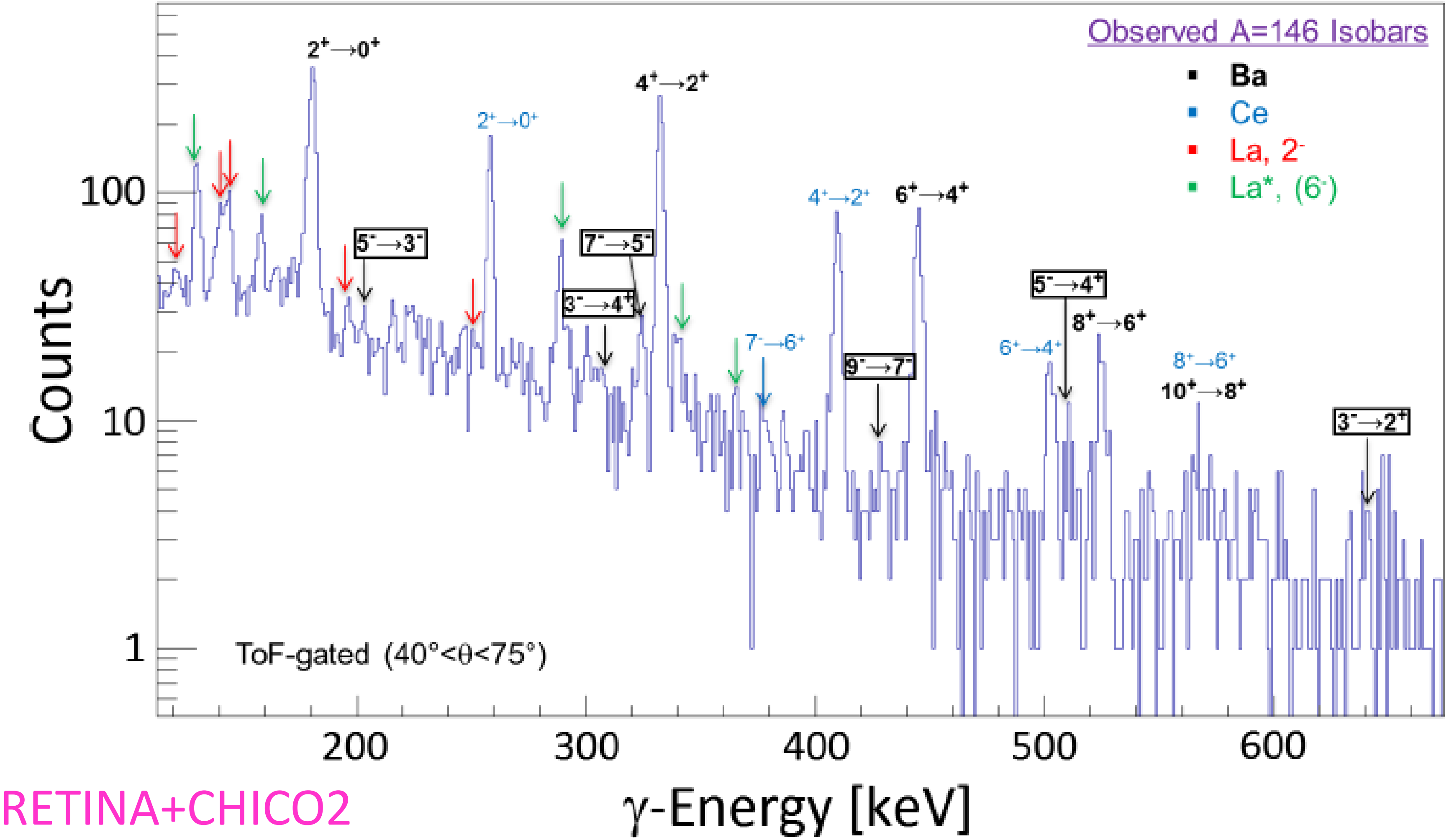

CARIBU+GRETINA+CHICO2

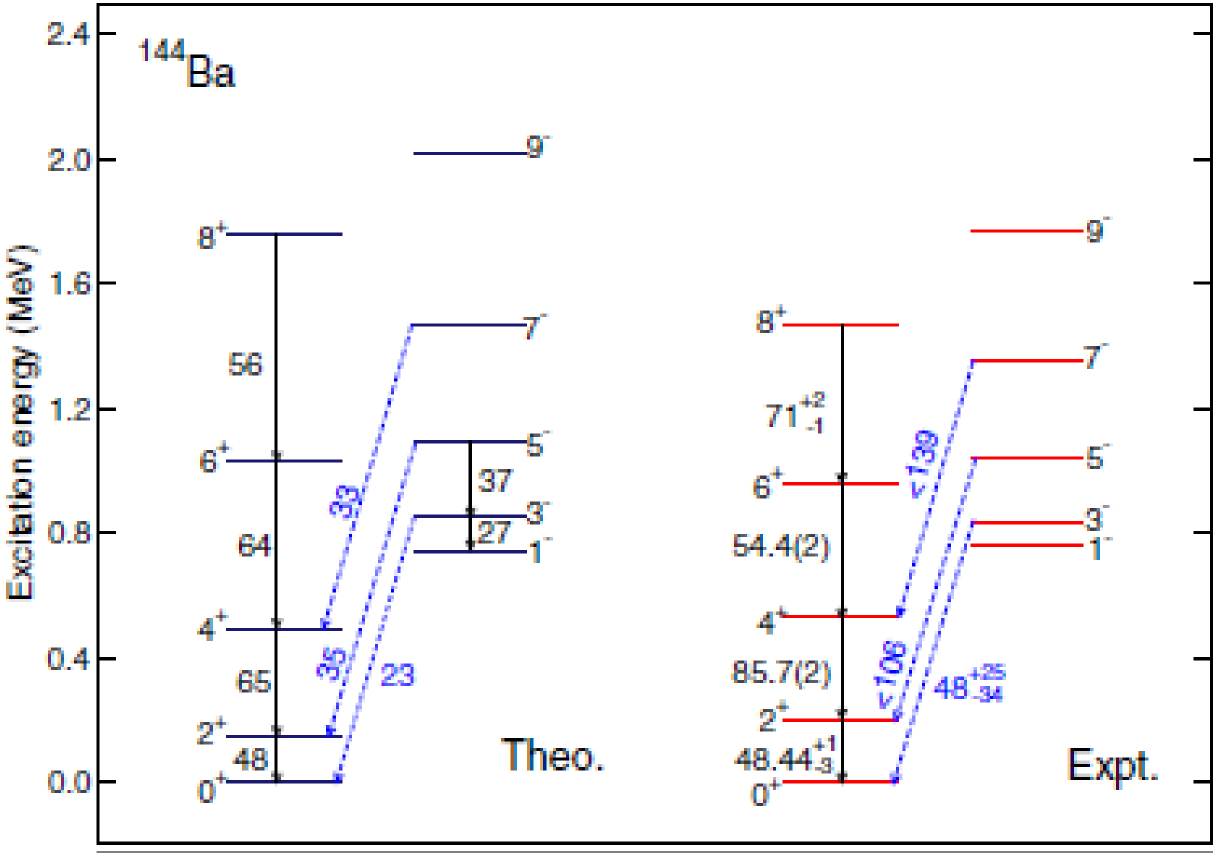

Theory for octupole-deformed Ba nuclei

PHYSICAL REVIEW C 97, 024317 (2018)

Signatures of octupole correlations in neutron-rich odd-mass barium isotopes

K. Nomura, T. Nikšić, and D. Vretenar

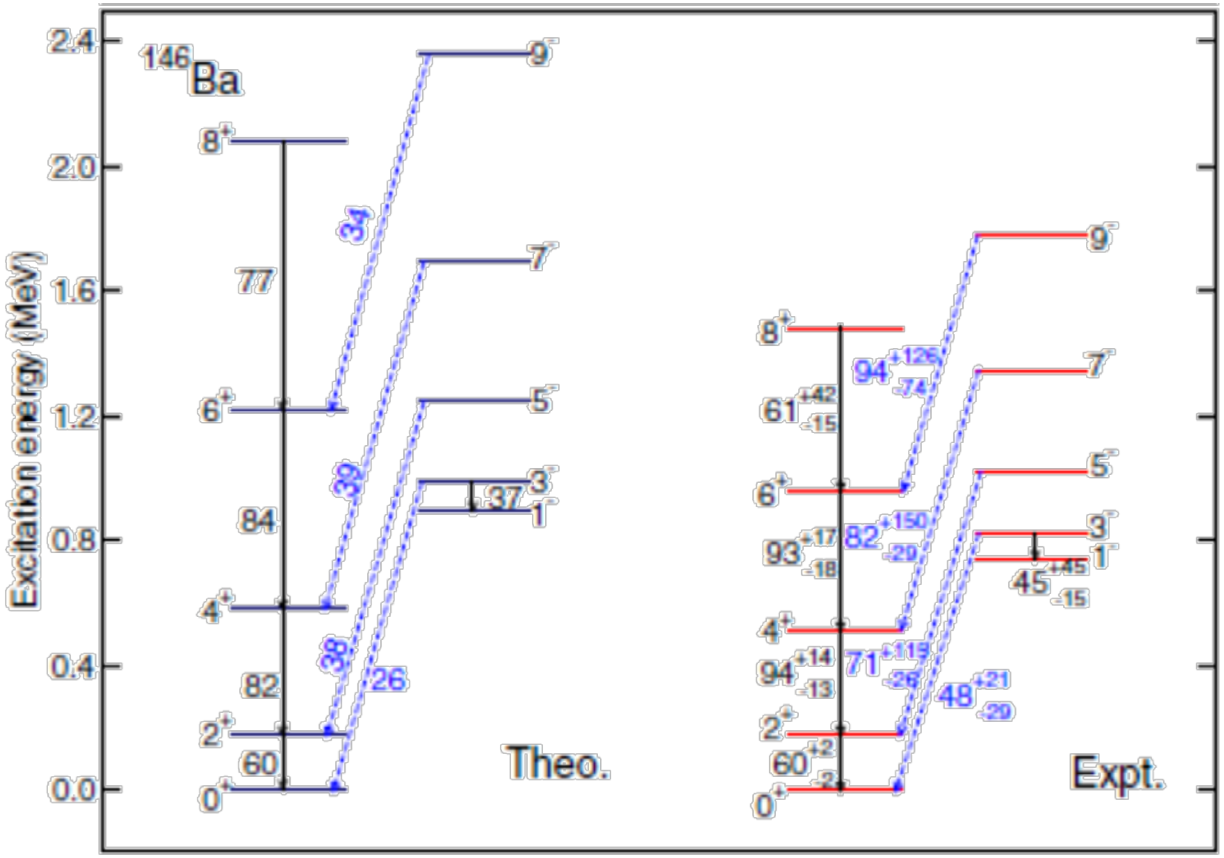

Note positive and negative parity rotational sequences, with cross-transitions

Combining Coulomb and nuclear scattering

PHYSICAL REVIEW C **79**, 011302(R) (2009)

Persistent decoupling of valence neutrons toward the dripline: Study of ^{20}C by γ spectroscopy

Z. Elekes,[1] Zs. Dombrádi,[1] T. Aiba,[2] N. Aoi,[3] H. Baba,[3] D. Bemmerer,[4] B. A. Brown,[5] T. Furumoto,[6] Zs. Fülöp,[1] N. Iwasa,[7] Á. Kiss,[8] T. Kobayashi,[7] Y. Kondo,[9] T. Motobayashi,[3] T. Nakabayashi,[9] T. Nannichi,[9] Y. Sakuragi,[3,6] H. Sakurai,[3] D. Sohler,[1] M. Takashina,[10] S. Takeuchi,[3] K. Tanaka,[3] Y. Togano,[11] K. Yamada,[3] M. Yamaguchi,[3] and K. Yoneda[3]

Coulomb Excitation

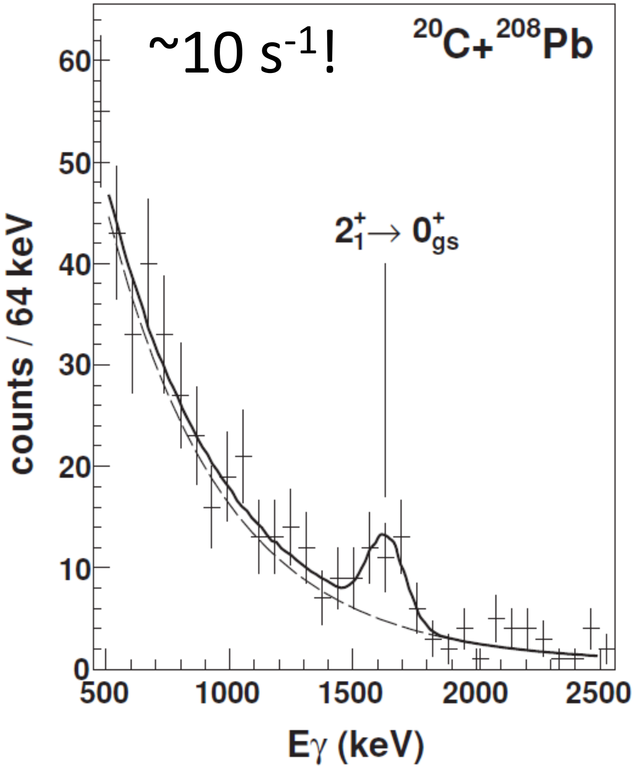

Nuclear Excitation

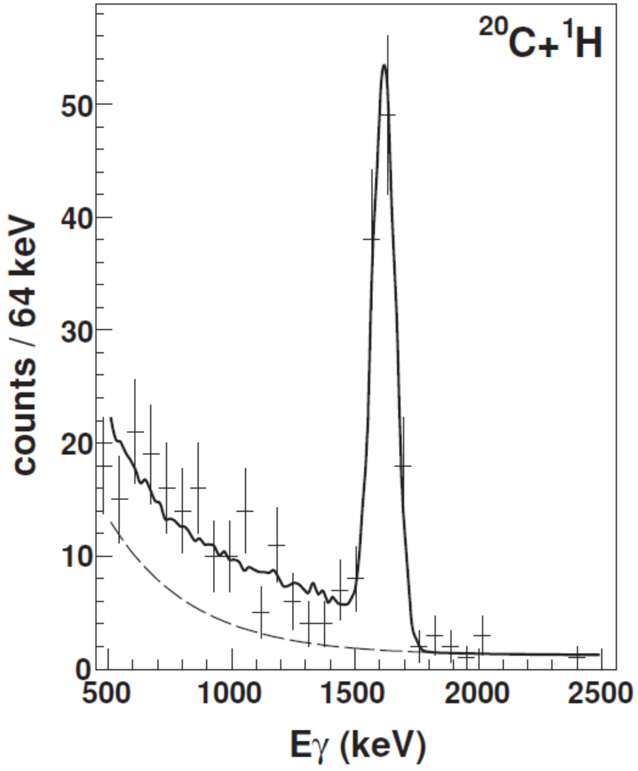

M_p and M_n

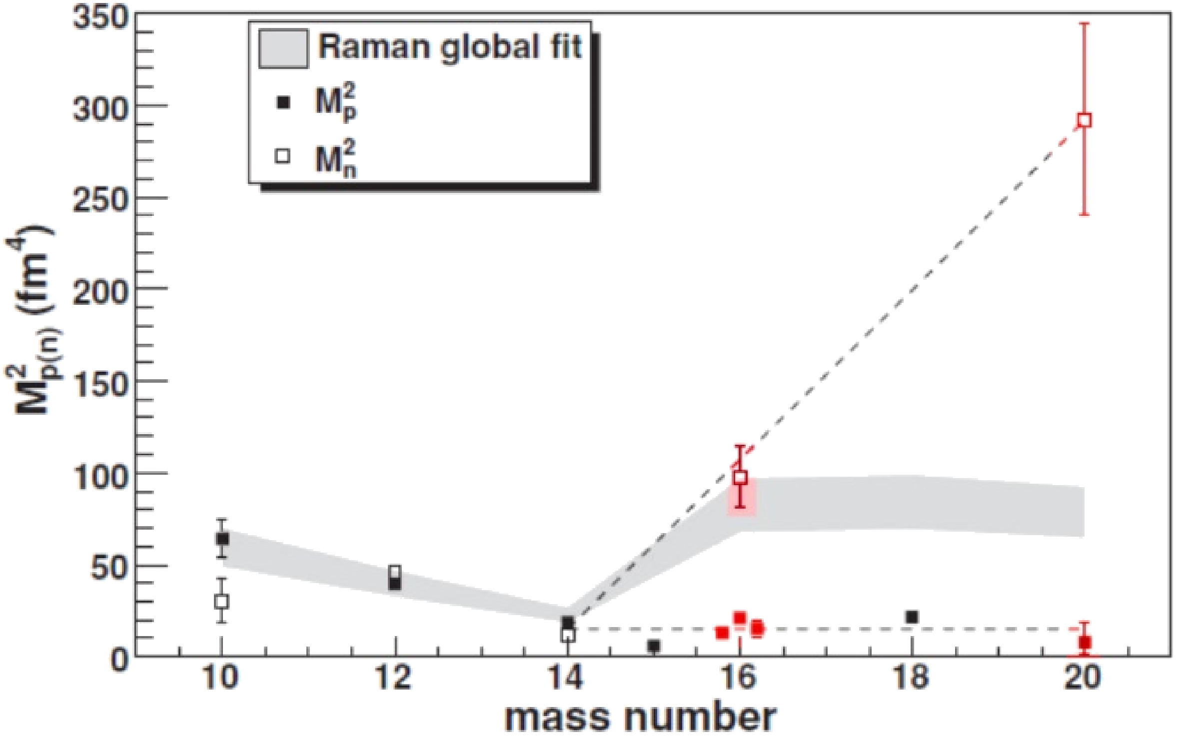

Conclusions

- Simple scattering reactions can already inform us about nuclear structure
- Since cross sections tend to be large, these can be extremely useful if the intensity of the beam is small
- We should understand scattering reactions before we turn to the more complex problem of extracting nuclear-structure information from re-arrangement (transfer) reactions.